ARTICLE OPEN

Check for updates

Microwave mode cooling and cavity quantum electrodynamics effects at room temperature with optically cooled nitrogen-vacancy center spins

Yuan Zhang[1]✉, Qilong Wu[1], Hao Wu[2,3], Xun Yang[1], Shi-Lei Su[1], Chongxin Shan[1]✉ and Klaus Mølmer[4,5]✉

Recent experimental and theoretical studies demonstrated microwave mode cooling and cavity quantum electrodynamics (C-QED) effects at room temperature by using optically cooled nitrogen-vacancy (NV) spins. In this article, we consider improvements of these effects by exploring parameters in recent diamond maser experiments with a high frequency microwave resonator. By accounting for the rich electronic and spin levels, we provide a more complete treatment of optical pumping and dissipation in NV centers, and study the dependence of system performance on laser power. We predict the reduction of microwave photon number down to 261 (equivalent to a temperature of 116 K), about five times lower than the values reported recently. We also predict the laser-power controlled C-QED effects across weak-to-strong coupling regimes, and observe saturation of these effects under strong laser pumping. Our model can be modified straightforwardly to investigate similar effects with other solid-state spins and possible C-QED effects in maser operation.

npj Quantum Information (2022)8:125 ; https://doi.org/10.1038/s41534-022-00642-z

INTRODUCTION

Nitrogen vacancy (NV) centers in diamond constitute a prototypical solid-state spin system[1] with many applications, such as sensing of magnetic fields[2,3], electric fields[4], local strain[5], temperature[6], and quantum processing and computation[7,8]. These applications benefit from unique properties of the NV centers, namely, a spin-1 triplet electronic ground state with long coherence time at room temperature, and easy initialization and readout of the spin states by optical means.

Polarization of the NV spins by optical pumping is usually applied as the first step in optical detection of magnetic resonance experiments. Recently, Ng W. et al.[9] suggested that this polarization is equivalent to cooling of NV spin ensemble, and the cooled spin ensemble can be applied to cool a coupled microwave mode. In experiment, they demonstrated the cooling of a microwave resonator with 2.87 GHz frequency from 293 K (room temperature) to 188 K. In contrast to conventional cooling with bulky dilution refrigerators, this cooling mechanism can be achieved with a bench-top device in a room temperature laboratory environment. A sufficiently cooled microwave mode may approach pure quantum states and permit study of quantum entanglement[10], quantum gate operations[11] and quantum thermodynamics[12], and it can also improve the measurement sensitivity in electron and nuclear spin resonance experiments[3,13]. Inspired by the unambiguous demonstration of cavity quantum electrodynamics (C-QED) effects with the triplet spins of pentacene molecules at room temperature[14], we showed in a recent publication[15], that optically cooled NV spins permit the realization of C-QED effects at room temperature, such as Rabi oscillations, Rabi splittings and stimulated superradiance.

So far, microwave mode cooling by NV center spins was limited by the weak spin-microwave mode coupling as compared with the large spin-dephasing rate and the high ambient excitation of the low frequency microwave mode. In this article, we propose to study the setup shown in Fig. 1, where a magnetic field Zeeman-splits the NV spin levels, and the resulting 9.22 GHz $0 \rightarrow +1$ spin transition couples resonantly to a dielectric microwave resonator. Although the proposed scheme could work with any high frequency, to ensure the immediate applicability of our results we assume a resonator with 9.22 GHz frequency and 1.88 MHz photon damping rate as the one used in the experiment of Breeze J. D. et al.[16] Different from our proposal, that experiment explored the population-inverted $-1 \rightarrow 0$ spin transition, and achieved continuous maser operation at 9.22 GHz frequency, which matches the frequency of cesium atomic clocks and may thus be used in quantum metrology.

In comparison to the experiment[9], in our proposed setup, the number of thermal photons n_{th}^{m} inside the resonator is reduced by about a factor three because of the three times higher mode frequency, while the photon damping rate κ is about three times smaller, which together reduces the photon thermalization rate κn_{th}^{m} by an order of magnitude. In addition, the rate of energy transfer from the resonator to the NV spins is three times larger as it is also proportional to the square of the spin-resonator coupling, which is proportional to the square root of the mode frequency[16]. In summary, our proposed setup enhances the energy transfer rate and suppresses the field thermalization rate, which together improve the performance of the microwave mode cooling.

[1]Henan Key Laboratory of Diamond Optoelectronic Materials and Devices, Key Laboratory of Material Physics, Ministry of Education, School of Physics and Microelectronics, Zhengzhou University, Daxue Road 75, Zhengzhou 450052, China. [2]Center for Quantum Technology Research and Key Laboratory of Advanced Optoelectronic Quantum Architecture and Measurements (MOE), School of Physics, Beijing Institute of Technology, 100081 Beijing, China. [3]Beijing Academy of Quantum Information Sciences, 100193 Beijing, China. [4]Center for Complex Quantum Systems, Department of Physics and Astronomy, Aarhus University, Ny Munkegade 120, DK-8000 Aarhus C, Denmark. [5]Aarhus Institute of Advanced Studies, Aarhus University, Høegh-Guldbergs Gade 6B, DK-8000 Aarhus C, Denmark. ✉email: yzhuaudipc@zzu.edu.cn; cxshan@zzu.edu.cn; moelmer@phys.au.dk

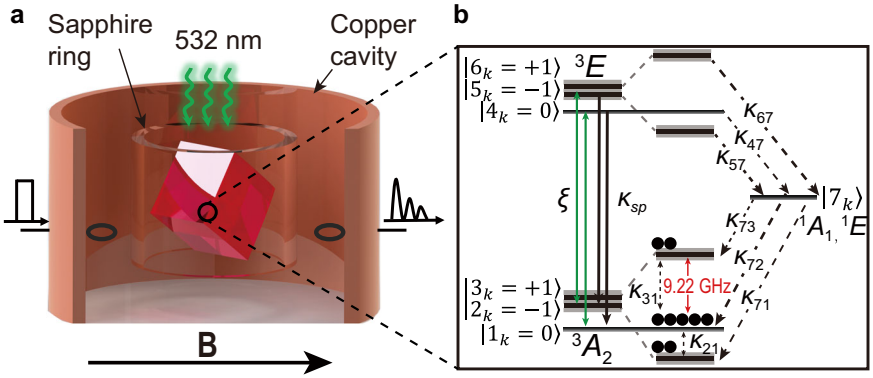

Fig. 1 Proposed system and energy diagram. a Setup modified from the diamond maser experiment[16] with nitrogen-vacancy (NV) centers in diamond excited by a 532 nm laser and coupled to a single-crystal sapphire dielectric ring microwave resonator inside a copper cylindrical cavity in the presence of a magnetic field, where the resonator is driven by a microwave field and the transmitted signal is measured. **b** Downward and upward Zeeman shift of the spin levels with projections −1 and +1, and the processes involving the multiple electronic and spin levels of the NV centers: optical excitation and stimulated emission with rate ξ (green double-headed arrows), spontaneous emission with rate k_{sp} (downward black arrows), inter-system crossing with rates k_{i7}, k_{7j} (with $i=4,5,6$ and $j=1,2,3$, tilted dashed arrows), spin-lattice relaxation with rates $k_{31}\approx k_{13}$, $k_{21}\approx k_{12}$ (double-head dashed arrows), and spin-dephasing with rates χ_2, χ_3 (shaded gray width of energy levels). The thickness of arrows indicates the relative amplitude, and the black spheres show the relative population of the three spin levels on the electronic ground state. The values of various rates are specified in the Supplementary Table 1, and more details are provided in the main text.

In the following, firstly, we go beyond the standard Jaynes–Cumming (JC) model for many two-level systems to account for all the electronic and spin levels of NV centers, see Fig. 1b. This allows a more precise description of the optical spin cooling and the NV spin-resonator collective coupling, as compared to the simplified, effective two-level model in our previous study[15]. Furthermore, we manage to simulate trillions of NV centers by solving our extended model with a mean-field approach[17–19]. In this treatment we include the spin-photon and spin-spin quantum correlations by a second-order mean-field approach, which are important to deal with the collective effects properly.

Then, we investigate the influence of the laser excitation on the evolution of the ground state spin-level populations and the cooling of the microwave mode. Our calculations predict a reduction of the microwave photon number to 261 (equivalent to a temperature of 116 K), which is about five times smaller than the results obtained so far with NV centers[9]. Within the more complete model, the spin-spin correlations are shown to be responsible for a higher final temperature than obtained from a simpler rate equation treatment, which yields 87 K for otherwise similar parameters.

Finally, we study how the laser power controls the NV spins-microwave mode collective coupling, and the resulting Rabi oscillations and splitting effects. Our calculations indicate that the saturation of the optical transition limits the strength of the collective coupling, and a larger number of NV spins may be required to fully demonstrate C-QED effects at room temperature. In the end, we summarize our conclusions and comment on possible extensions for future exploration.

RESULTS

Multi-level Jaynes–Cumming (JC) model

In the following, we present the multi-level JC model for the system shown in Fig. 1. We consider the quantum master equation for the reduced density operator $\hat{\rho}$ of the coupled NV centers-microwave resonator system:

$$\begin{aligned}\partial_t\hat{\rho} = &-\tfrac{i}{\hbar}\left[\hat{H}_{NV}+\hat{H}_m+\hat{H}_{NV-m}+\hat{H}_{m-m},\hat{\rho}\right]\\ &-\xi\sum_k\left(\mathcal{D}\left[\hat{\sigma}_k^{41}\right]\hat{\rho}+\mathcal{D}\left[\hat{\sigma}_k^{52}\right]\hat{\rho}+\mathcal{D}\left[\hat{\sigma}_k^{63}\right]\hat{\rho}\right)\\ &-\left(\xi+k_{sp}\right)\sum_k\left(\mathcal{D}\left[\hat{\sigma}_k^{14}\right]\hat{\rho}+\mathcal{D}\left[\hat{\sigma}_k^{25}\right]\hat{\rho}+\mathcal{D}\left[\hat{\sigma}_k^{36}\right]\hat{\rho}\right)\\ &-\sum_k\left(\sum_{i=4,5,6}k_{i7}\mathcal{D}\left[\hat{\sigma}_k^{7i}\right]\hat{\rho}+\sum_{i=1,2,3}k_{7i}\mathcal{D}\left[\hat{\sigma}_k^{i7}\right]\hat{\rho}\right)\\ &-\sum_k\sum_{i=2,3}\left(k_{i1}\mathcal{D}\left[\hat{\sigma}_k^{1i}\right]\hat{\rho}+k_{1i}\mathcal{D}\left[\hat{\sigma}_k^{i1}\right]\hat{\rho}+2\chi_i\mathcal{D}\left[\hat{\sigma}_k^{ii}\right]\hat{\rho}\right)\\ &-\kappa\left[\left(n_m^{th}+1\right)\mathcal{D}[\hat{a}]\hat{\rho}+n_m^{th}\mathcal{D}\left[\hat{a}^\dagger\right]\hat{\rho}\right].\end{aligned}\tag{1}$$

We consider the multiple levels of the k-th NV center as shown in Fig. 1b, and denote the three spin levels (with projection $0,-1,+1$) of the triplet ground state $^3A_2$ as the levels $|1_k\rangle,|2_k\rangle,|3_k\rangle$, and those of the triplet excited state ^3E as the levels $|4_k\rangle,|5_k\rangle,|6_k\rangle$, and introduce a fictitious level $|7_k\rangle$ to effectively represent the two singlet excited states $^1A_1$,^1E[9]. The NV centers are described by the Hamiltonian $\hat{H}_{NV}=\hbar\omega_{31}\sum_{k=1}^{N}\hat{\sigma}_k^{31}\hat{\sigma}_k^{13}$ with the transition frequency ω_{31} between the $|1_k\rangle$ and $|3_k\rangle$ level. Here and in the following, the symbols $\hat{\sigma}_k^{ij}=|i_k\rangle\langle j_k|$ represent projection operators (with $i=j$) or transition operators (with $i\neq j$). The transitions between other levels are not considered in the Hamiltonian, but through the dissipative super-operators as discussed below. The microwave resonator is described by the Hamiltonian $\hat{H}_m=\hbar\omega_m\hat{a}^\dagger\hat{a}$ with the frequency ω_m, the photon creation $\hat{a}^\dagger$ and annihilation operator $\hat{a}$, respectively. The energy exchange between the NV centers and the microwave resonator mode is described by the Hamiltonian $\hat{H}_{NV-m}=\hbar g_{31}\sum_k(\hat{a}^\dagger\hat{\sigma}_k^{13}+\hat{\sigma}_k^{31}\hat{a})$ with the coupling strength g_{31}.

The Hamiltonian $\hat{H}_{m-m} = \hbar\Omega\sqrt{\kappa/2}\hat{a}e^{i\omega_d t} + h.c.$ describes the driving of the microwave mode by a microwave field of frequency ω_d and driving strength Ω, where $\sqrt{\kappa/2}$ is the assumed amplitude transmission coefficient through the coupler (with the resonator photon decay rate κ).

The remaining terms in Eq. (1) describe the system dissipation with the Lindblad superoperator $\mathcal{D}[\hat{o}]\hat{\rho} = \frac{1}{2}\left\{\hat{o}^\dagger\hat{o}, \hat{\rho}\right\} - \hat{o}\hat{\rho}\hat{o}^\dagger$ for any operator $\hat{o}$. The second line describes the optical pumping with a rate ξ from the spin levels of the triplet ground state to those of the triplet excited state. The third line describes the stimulated emission with the same rate ξ and the spontaneous emission with a rate k_{sp} from the spin levels of the triplet excited state to those of the triplet ground state. The fourth line describes the inter-system crossing with rates k_{47}, k_{67}, k_{57} from the spin levels of the triplet excited state to the representative singlet excited state[9], and describes the similar process with rates k_{73}, k_{72}, k_{71} from the singlet excited state to the spin levels of the triplet ground state. The fifth line describes the spin-lattice relaxation with rates k_{31}, k_{12} from the $+1, -1$ spin levels to the 0 spin level on the triplet ground state, and with the rates $k_{13} \approx k_{31}, k_{21} \approx k_{12}$ for the reverse processes, as well as the spin dephasing with the rates χ_3, χ_2 of the $+1, -1$ spin levels. The spin-lattice relaxation is dominated by one photon processes at extremely low temperatures[20], and by two-phonon Raman scattering and the Orbach process at room temperature with $k_{31} \approx k_{12}$[21,22]. To keep the model tractable, we use a single dephasing rate to model qualitatively the spin dephasing due to the coupling with the spin environment, and the decoherence due to inhomogeneous broadening of spin transitions. The last line describes the thermal photon emission and absorption of the resonator mode with the rate κ and the thermal photon number $n_m^{th} = \left[e^{\hbar\omega_m/k_BT} - 1\right]^{-1}$ at temperature T (with the Boltzman constant k_B). The value of various rates and the calculation of ξ from the laser power P are specified in the Supplementary Note 1.

To simulate trillions of NV centers, we solve the quantum master Eq. (1) with the mean-field approach[23]. In this approach, we derive the equation $\partial_t\langle\hat{o}\rangle = \mathrm{tr}\{\hat{o}\partial_t\hat{\rho}\}$ for the expectation values $\langle\hat{o}\rangle = \mathrm{tr}\{\hat{o}\hat{\rho}\}$ of any operator $\hat{o}$, and truncate the resulting equation hierarchy by approximating the mean values of products of many operators with those of few operators, i.e. the cumulant expansion approximation. In Eq. (1), we assume the same transition frequencies ω_{31}, coupling strength g_{31} and rates $\xi, k_{sp}, k_{ij}, \chi_2, \chi_3$ for all the NV centers, which allows us to utilize the symmetry raised to reduce dramatically the number of independent mean-field quantities. We utilize the QuantumCumulant.jl package[23] to derive and solve the equations for the mean-field quantities up to second order, see the Supplementary Fig. 1. In the Supplementary Note 3, we consider the system without the microwave field driving, and present the derived equations for the population $\langle\hat{\sigma}_1^{ii}\rangle$ of the i-th level, the mean intra-resonator photon number $\langle\hat{a}^\dagger\hat{a}\rangle$, the spin-photon correlation $\langle\hat{a}^\dagger\hat{\sigma}_1^{31}\rangle$ and the spin-spin correlation $\langle\hat{\sigma}_1^{31}\hat{\sigma}_2^{13}\rangle$. Here, the sub-index 1 or 1, 2 indicate the mean-quantities for the first and second representative NV centers.

Cooling of NV spin ensemble and microwave mode

We apply the multi-level JC model to study firstly the optical spin cooling and the resulting cooling of the microwave mode, by considering the system dynamics under a laser pulse excitation (Fig. 2), and the system steady-state under continuous laser excitation (Fig. 3). To quantify the non-equilibrium state of the resonator, we define the effective temperature $T_{mode} = \hbar\omega_m/[k_B(1/\langle\hat{a}^\dagger\hat{a}\rangle + 1)]$ for the microwave mode such that a photon thermal bath at this temperature would have the same mean photon number.

Figure 2 shows the dynamics of the optical spin cooling and the subsequent microwave mode cooling. Before the laser excitation,

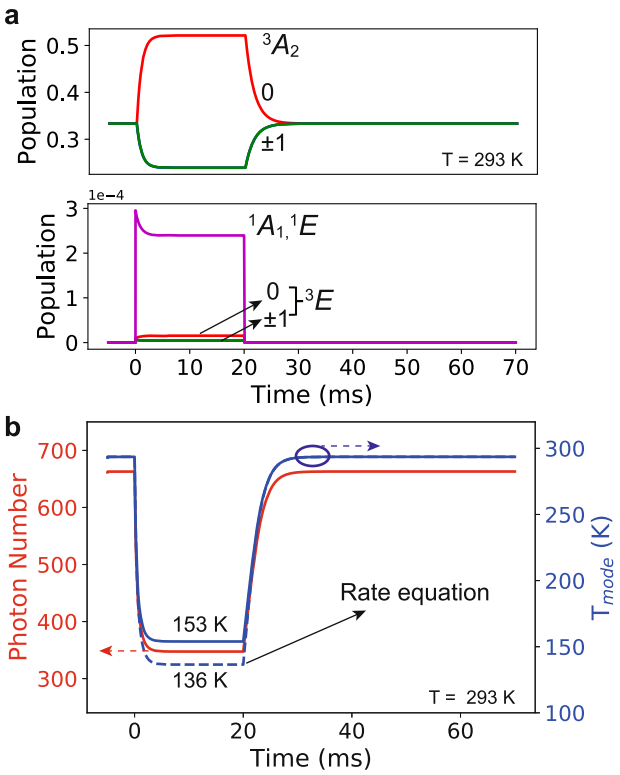

Fig. 2 Cooling dynamics of an NV spin ensemble and a microwave resonator mode. a Population of the spin levels of the electronic ground state (the upper panel), and the population of those of the electronic excited state and the representative singlet excited state (lower panel). **b** Intra-resonator photon number (red solid line, left axis) and the effective mode temperature (right axis) calculated with the multi-level JC model (blue solid line) and the rate equations (blue dashed line). Here, the diamond is illuminated by a 532 nm laser with 2 W power and 20 ms duration, and there is no microwave driving field. Other parameters are specified in the Supplementary Table 1.

the population is equally split among the three spin levels of the triplet ground state (Fig. 2a), and the mean photon number in the resonator is around the thermal value 661 (red curve in Fig. 2b). The effective temperature of the microwave mode is equal to the room temperature 293 K.

When the laser excitation is on, the population of the 0 spin level of the triplet ground state first increases and then converges slowly to a constant value of 0.52, while the populations of the -1 and $+1$ spin levels first decrease fast and then converge slowly to the constant values of 0.24 (upper part of Fig. 2a). The population of the spin levels of the triplet excited state increases dramatically and then behaves similarly as that of the spin levels of the triplet ground state except for the four orders of magnitude smaller value, while the singlet excited state accumulates about fifty times larger population than the triplet excited state (lower part of Fig. 2a). During this dynamics, the mean photon number drops dramatically and converges within 20 ms to a value below 347, equivalent to a reduction of the effective microwave mode temperature by 140 K, from 293 K to 153 K (red and blue solid line in Fig. 2b).

When the laser excitation is turned off, the populations of the ±1 and 0 spin level of the triplet ground state evolve back to their initial values within about 10 ms (upper part of Fig. 2a), and the population of the optically excited levels reduces rapidly to zero (lower part of Fig. 2a). The mean photon number returns slowly to its initial value, and the effective mode temperature returns to room temperature (Fig. 2b). These results are qualitatively similar to those observed in the experiment[9] (see the Supplementary Fig. 2).

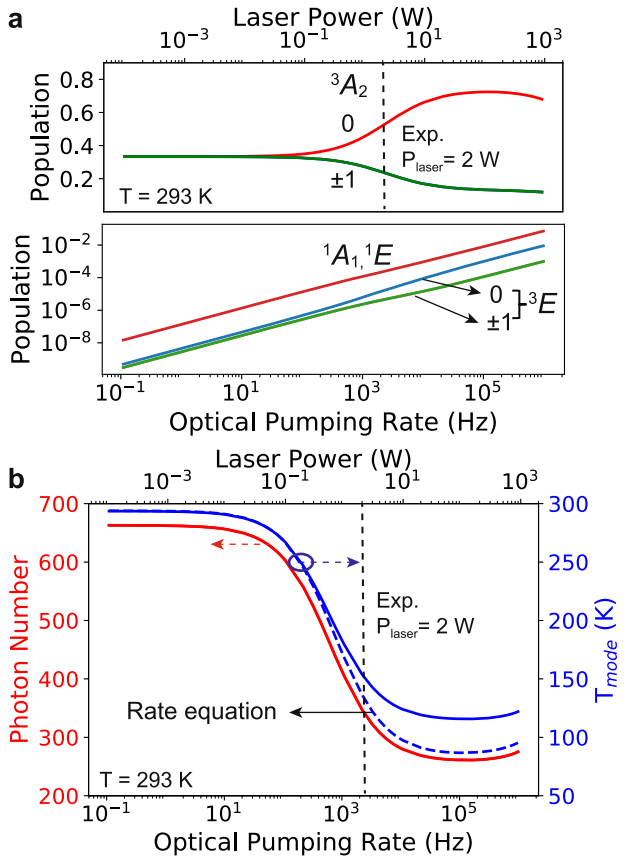

Fig. 3 Steady-state cooling of the NV spins and the microwave resonator mode. a, **b** Steady-state values of the same quantities as shown in Fig. 2a, b as function of the optical pumping rate ξ (lower axis) or the laser power (upper axis). The laser power 2 W, as used in Fig. 2 and the experiment[9], is marked with the vertical dashed line. There is no microwave driving field, and other parameters are specified in the Supplementary Table 1.

To gain more insights into the above results, we assume the vanishing of the correlation $\langle\hat{\sigma}_1^{31}\hat{\sigma}_2^{13}\rangle \approx 0$ between different spins, and eliminate the spin-photon correlation $\langle\hat{a}^\dagger\hat{\sigma}_1^{31}\rangle$ adiabatically to arrive at rate equations for the population of the NV levels and the intra-resonator photon number (see the Supplementary Note 5). These rate equations reproduce the dynamics shown in Fig. 2 qualitatively, but yields a photon number of 307 and an effective mode temperature of 136 K (see the blue dashed line in Fig. 2b), which is about 17 K lower than the value obtained by the full calculations. Note that for the setup in the weak coupling regime as in the experiment[9], the rate equations reproduce the results of the full multi-level JC model (see the Supplementary Note 4).

According to the rate equations, the intra-cavity photon number follows the equation

$$\partial_t\langle\hat{a}^\dagger\hat{a}\rangle \approx \kappa\left(n_m^{th} - \langle\hat{a}^\dagger\hat{a}\rangle\right) - Nk_{eet}(\langle\hat{\sigma}_1^{11}\rangle - \langle\hat{\sigma}_1^{33}\rangle)\langle\hat{a}^\dagger\hat{a}\rangle, \quad (2)$$

where the first and second term describe the thermalization, the stimulated absorption and emission of microwave photons, respectively. Here, we have ignored the negligible spontaneous emission of the photons, and introduced the energy transfer rate $k_{eet} \approx \frac{g_{31}^2\chi}{(\omega_m-\omega_{31})^2+\chi^2/4}$ with the total decay rate $\chi \approx \kappa + 2\chi_3$. Equation (2) indicates that we should either reduce the thermalization rate κn_m^{th}, or increase the number of NV centers N, the energy transfer rate k_{eet}, and the population difference $\langle\hat{\sigma}_1^{11}\rangle - \langle\hat{\sigma}_1^{33}\rangle$ in order to achieve the better microwave mode cooling. In the present article, we have essentially reduced n_m^{th}, and increased k_{eet} (via g_{31}) by exploring the microwave resonator with higher frequency, and increased $\langle\hat{\sigma}_1^{11}\rangle - \langle\hat{\sigma}_1^{33}\rangle$ by exploring the strong laser pumping, see below.

Figure 3 shows the steady-state cooling performance for different optical pumping rates (laser powers). We find that the population of the 0 (±1) spin level of the triplet ground state increases (decreases) when the optical pumping rate (laser power) exceeds about 100 Hz (9.1×10^{-2} W), and saturates at about 0.73 (0.13) for an optical pumping rate about 10^5 Hz (100 W). For even stronger optical pumping (higher laser power), the population of all these levels decrease, as the populations of the triplet and singlet excited levels increase with increasing optical pumping rate (see the upper and lower parts of Fig. 3a). We observe also that the population of the 0 spin level of the triplet excited state becomes larger than that of the ±1 spin levels once the optical pumping rate (laser power) exceeds 100 Hz (9.1×10^{-2} W), see the lower part of Fig. 3a.

Accompanying the changes of spin level populations, the intra-resonator photon number decreases dramatically when the optical pumping rate (laser power) exceeds 100 Hz (9.1×10^{-2} W), and approaches a minimum about 261 for an optical pumping rate (laser power) about 10^5 Hz (10^2 W), which is about five times smaller than the values reported before[9]. The mean number of photons in the resonator increases weakly for much stronger optical pumping, see Fig. 3b. Equivalently, the effective mode temperature decreases from room temperature to a minimum around 116 K, which is 72 K lower than values achieved so far[9]. As above, effective rate equations result to the similar results except for slightly lower temperatures (blue dashed line in Fig. 3b). In our simulations, if we increase the number of NV centers by a factor 40 to the same level 1.6×10^{15} as in the experiment[9], we obtain a more efficient cooling of the microwave mode and achieve a steady-state mean photon number of 71, corresponding to an effective temperature as low as 32 K (not shown).

Laser power-controlled C-QED effects

In the above simulations, we demonstrated that the optically cooled NV spin ensemble can be used to cool the microwave mode. In the following, we demonstrate that it can be also utilized to realize the collective strong coupling with the cooled microwave mode, and to manifest the C-QED effects in a room temperature environment. These effects have been studied previously[15] within a simpler model, which treats the NV spins as two-level systems and employs a single spin relaxation rate for the optical spin cooling. Here, with the more advanced model, we provide more precise and quantitative estimates, and explore extra effects due to the higher excited levels of NV centers, which should be able to guide directly the experimental research in future.

We employ the average of Dicke states numbers J, M to illustrate the collective coupling of the NV spin ensemble to the microwave resonator. As explained in[15], J, M quantify the symmetry of the Dicke states (and the collective coupling strength) and the degree of excitation, respectively, and the allowed values of these numbers form a triangular space enclosed by the dashed lines, as shown in Fig. 4a. In the Supplementary Note 2, we explain the prescript to calculate the mean of these numbers with the spin level populations and the spin-spin correlations. Alternatively, according to ref. [24], we can also estimate roughly the mean Dicke states numbers through $M = J_0(2p-1), J(J+1) = (2p-1)^2J_0(J_0+1) + 6p(p-1)J_0$ with $J_0 = N/2$ and p denoting the population on the upper spin level coupled resonantly to the microwave resonator. For the current system with multiple levels, we apply the ratio of populations $p = \langle\hat{\sigma}_1^{33}\rangle/(\langle\hat{\sigma}_1^{11}\rangle + \langle\hat{\sigma}_1^{33}\rangle)$ obtained with the multi-level JC model, to evaluate the averaged numbers J, M. In Fig. 4a, we display the steady-state values of these numbers normalized to the number of NV centers N for different values of the laser power. We see that as the laser power

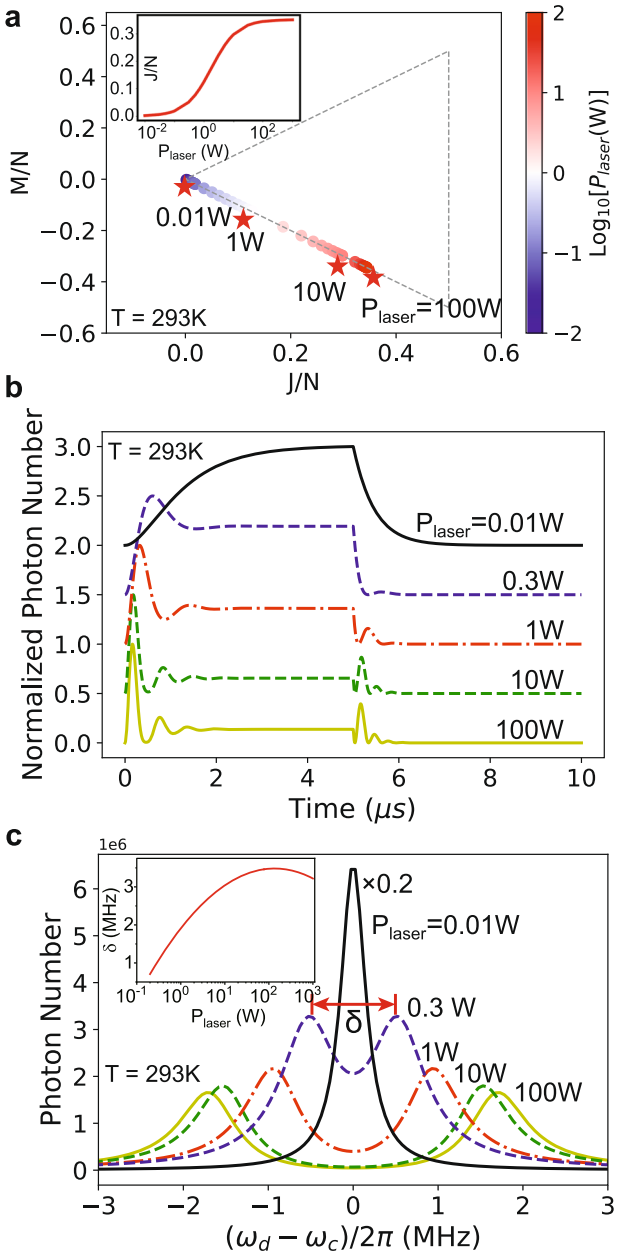

Fig. 4 Room-temperature C-QED effects with NV center spins coupled to a 532 nm laser field and a microwave resonator field mode. a Representation of the $+1, 0$ spin level steady-state populations and spin-spin correlations by the average of the Dicke state quantum numbers J, M (normalized by the total number N of NV centers) for different values of the laser power. The gray dashed lines indicate the boundary of the Dicke state space. The inset shows J/N as a function of laser power. **b**, **c** Dynamics of the normalized intra-resonator photon number for the system driven resonantly by a pulsed microwave field of duration 5 μs and strength $\Omega = 2\pi \times 9.7 \times 10^5\,\mathrm{Hz}^{-1/2}$ (**b**), and the steady-state intra-resonator photon number for the system driven by a continuous-wave microwave field as a function of the detuning of the microwave driving field frequency ω_d and the microwave resonator frequency ω_c (**c**), where the diamond is illustrated by a 532 nm laser with increasing power 0.01, 0.3, 1, 10, 100 W. In **b**, the curves are shifted vertically for the sake of clarity. The inset of **c** shows the Rabi splitting δ as a function of the laser power. Here, we have considered the system with ten times more NV centers than that used in the experiment[16].

increases from 10^{-2} W to 1 W and finally to 100 W, the NV spin ensemble starts from the Dicke state on the leftmost corner with small J and low symmetry, and evolves along the lower boundary towards Dicke states with larger $J/N \approx 0.35$ and higher symmetry. The population saturation as revealed before prevents the system from reaching the fully symmetric Dicke states with $J = N/2$ on the rightmost corner. In the inset of Fig. 4a, we summarize these behaviors by showing the mean number J as a function of the laser power.

Since the NV spin ensemble-microwave mode coupling scales as $\propto \sqrt{2J}g$, we expect that the coupling increases with laser power. For $N = 4 \times 10^{13}$ centers as used in the diamond maser experiment[16], we estimate the largest coupling strength as $\sqrt{2J}g \approx 2\pi \times 0.57$ MHz, which is slightly smaller than the spin-dephasing rate $\chi 3 = 2\pi \times 0.64$ MHz, and conclude that the system is at the edge of the strong coupling regime. Thus, to demonstrate C-QED effects at room temperature, it would be beneficial to increase the number of NV centers and the single spin-microwave mode coupling, or decrease the spin-dephashing rate and the photon damping rate. As suggested in refs. [2,25], by reducing the ^{13}C concentration, we can obtain diamond sample with the same spin-dephasing rate but several times larger number of NV centers, see detailed discussion in the Supplementary Note 1. Thus, with an isotopically pure diamond sample, we may obtain ten times more NV spins, i.e. $N = 4 \times 10^{14}$, and achieve a collective coupling $\sqrt{2J}g \approx 2\pi \times 1.8$ MHz, which is now larger than the spin-dephasing rate and thus brings the system into the strong coupling regime.

For the system with more spins, it is possible to observe Rabi oscillations, see Fig. 4b. Here, we assume constant laser illumination (of different power 0.01, 0.3, 1, 10, 100 W) to cool the NV spin ensemble, and then apply a microwave field of a fixed amplitude for 5 μs, while studying the dynamics of the intra-resonator photon number. For the smallest laser power 0.01 W, the microwave photon number increases and then saturates when the microwave field is on, and it decreases exponentially when the driving field is off. For stronger laser power 0.3 W, the photon number shows a bump before reaching the saturation and the finite value. When the laser power increases further to 1 W and 10 W, the bump evolves into oscillations, and the oscillations become slightly faster. However, for much strong laser power 100 W, the oscillations do not change so much. These results are caused by the transition from the weak to strong collective coupling, enabled by the evolution of the spin ensemble from lower to higher symmetry Dicke states.

Alternatively, we can also investigate the Rabi splittings under continuous-wave microwave field driving, see Fig. 4c. Here, we study the intra-resonator mean photon number as a function of the frequency detuning of the driving field to the microwave resonator. For the smallest laser power 0.01 W, the photon number shows a single peak at zero detuning, and this peak evolves into two split peaks for larger laser power 0.3 W. The splitting δ of the peaks increases for much larger laser power 1 and 10 W, while it does not increase much further for even larger laser power 100 W. In the inset of Fig. 4c, we summarize these results by showing δ as a function of the laser power. By associating Fig. 4a, c, we find that the Rabi splitting can be used to infer the symmetry of the spin ensemble. By further linking Fig. 4a with Fig. 3, we expect that the Rabi splitting can be also applied to deduce the optical spin polarization and the microwave mode cooling. For strong laser power, the diamond might be heated, and, thus, in the Supplementary Note 6, we estimate the influence of the optical heating, and conclude that this influence can be mitigated by cooling the diamond sample with standard techniques.

DISCUSSION

In summary, we have proposed to cool the microwave resonator mode in a setup similar to that in the diamond maser experiment[16], which features a microwave resonator with high frequency and low photon damping rate, and stronger coherent coupling between the spins and the microwave mode. The improved parameters are beneficial for cooling the thermally excited microwave mode well below the ambient room temperature, and hence for observing C-QED effects (Rabi oscillations and mode splitting) in room temperature experiments. We presented a multi-level model to properly account for all details of the optical spin cooling and the collective NV spins-resonator coupling, and we investigated in detail the laser-power dependence of the level populations, the microwave mode cooling, and the spin ensemble states in the Dicke states space, the strength of the spin ensemble-resonator coupling, as well as the Rabi oscillations and splittings. By only minor modification, the model developed in this article can also describe NV spins coupled with nitrogen nuclear spin levels, and other solid-state spin systems, as well as investigate other interesting C-QED effects, e.g., in pulsed and continuous-wave masing. We note that, during preparation of this work, a preprint[26] in arXiv reported the experimental study on laser-power controlled microwave mode cooling, Rabi splittings with NV centers at room temperature, and the observation of saturation effects at strong laser power.

DATA AVAILABILITY

The authors declare that the main data supporting the finding of this study is available within the article and its Supplementary Information files. Additional data related to this paper is available from the corresponding authors upon reasonable request.

CODE AVAILABILITY

The authors declare that the basic codes to generate the numerical results in this study are explained within the Supplementary Information files.

Received: 7 April 2022; Accepted: 14 October 2022;
Published online: 02 November 2022

REFERENCES

1. Eisenach, E. R. et al. Cavity-enhanced microwave readout of a solid-state spin sensor. *Nat. Commun.* **12**, 1357 (2021).
2. Barry, J. F. et al. Sensitivity optimization for NV^- diamond magnetometry. *Rev. Mod. Phys.* **92**, 015004 (2020).
3. Taylor, J. M. et al. High-sensitivity diamond magnetometer with nanoscale resolution. *Nat. Phys.* **4**, 810–816 (2008).
4. Dolde, F. et al. Electric-field sensing using single diamond spins. *Nat. Phys.* **7**, 459–463 (2011).
5. Knauer, S., Hadden, J. P., & Rarity, J. G. In-situ measurements of fabrication induced strain in diamond photonic-structures using intrinsic colour centres. *npj Quantum Inf.* **6**, 50 (2020).
6. Kucsko, G. et al. Nanometre-scale thermometry in a living cell. *Nature* **500**, 54–58 (2013).
7. Wrachtrup, J. & Jelezko, F. Processing quantum information in diamond. *J. Phys. Condens. Matter*, **18**, S807–S824 (2006).
8. Tao, M. J., Hua, M., Ai, Q. & Deng, F. G. Quantum-information processing on nitrogen-vacancy ensembles with the local resonance assisted by circuit QED. *Phys. Rev. A* **91**, 062325 (2015).
9. Ng, W., Wu, H. & Oxborrow, M. Quasi-continuous cooling of a microwave mode on a benchtop using hyperpolarized NV^- diamond. *Appl. Phys. Lett.* **119**, 234001 (2021).
10. Haroche, S. & Raimond, J.-M. *Exploring the quantum: atoms, cavities, and photons* (Oxford, New York, 2006).
11. Henschel, K., Majer, J., Schmiedmayer, J. & Ritsch, H. Cavity QED with an ultracold ensemble on a chip: prospects for strong magnetic coupling at finite temperatures. *Phys. Rev. A* **82**, 033810 (2010).
12. Klatzow, J. et al. Experimental demonstration of quantum effects in the operation of microscopic heat engines. *Phys. Rev. Lett.* **122**, 110601 (2019).
13. Staudacher, T. et al. Nuclear magnetic resonance spectroscopy on a (5-nanometer)^3 sample volume. *Science* **339**, 561–563 (2013).
14. Breeze, J. D., Salvadori, E., Sathian, J., Alford, N. M. & Kay, C. W. M. Room-temperature cavity quantum electrodynamics with strongly coupled Dicke states. *npj Quantum Inf.* **3**, 40 (2017).
15. Zhang, Y. et al. Cavity quantum electrodynamics effects with nitrogen vacancy center spins coupled to room temperature microwave resonators. *Phys. Rev. Lett.* **128**, 253601 (2022).
16. Breeze, J. D., Salvadori, E., Sathian, J., Alford, N. M. N. & Kay, C. W. M. Continuous-wave room-temperature diamond Maser. *Nature* **555**, 493–496 (2018).
17. Debnath, K., Zhang, Y. & Mølmer, K. Lasing in the superradiant crossover regime. *Phys. Rev. A* **98**, 063837 (2018).
18. Zhang, Y., Shan, C. & Mølmer, K. Ultranarrow superradiant lasing by dark atom-photon dressed states. *Phys. Rev. Lett.* **126**, 123602 (2021).
19. Wu, Q. et al. A superradiant maser with nitrogen-vacancy center spins. *Sci. China Phys. Mech. Astron.* **65**, 217311 (2022).
20. Astner, T. et al. Solid-state electron spin lifetime limited by phononic vacuum modes. *Nat. Mater.* **17**, 313–317 (2018).
21. Norambuena, A. et al. Spin-lattice relaxation of individual solid-state spins. *Phys. Rev. B* **97**, 094304 (2018).
22. Jarmola, A., Acosta, V. M., Jensen, K., Chemerisov, S. & Budker, D. Temperature- and magnetic-field-dependent longitudinal spin relaxation in nitrogen-vacancy ensembles in diamond. *Phys. Rev. Lett.* **108**, 197601 (2012).
23. Plankensteiner, D., Hotter, C. & Ritsch, H. QuantumCumulants.jl: A Julia framework for generalized mean-field equations in open quantum systems. *Quantum.* **6**, 617 (2022).
24. Wesenberg, J. & Mølmer, K. Mixed collective states of many spins. *Phys. Rev. A* **65**, 062304 (2002).
25. Edmonds, A. M. et al. Characterisation of CVD diamond with high concentrations of nitrogen for magnetic-field sensing applications. *Mater. Quantum Technol.* **1**, 025001 (2021).
26. Fahey, D. P. et al. Steady-state microwave mode cooling with a diamond NV ensemble. Preprint at https://arxiv.org/abs/2203.03462 (2022).

ACKNOWLEDGEMENTS

This work was supported by the National Natural Science Foundation of China project No. 12004344, 62027816, 12274376, and Henan Center for Outstanding Overseas Scientists project No. GZS201903, Major Science and Technology Project of Henan Province grant No. 221100210400, the China Postdoctoral Science Foundation grant No. YJ20210035, 2021M700439, as well as the Danish National Research Foundation through the Center of Excellence for Complex Quantum Systems (Grant agreement No. DNRF156), and the European Union's Horizon 2020 Research and Innovation Programme under the Marie Sklodowska-Curie program (No. 754513).

AUTHOR CONTRIBUTIONS

Y.Z., C.S. and K.M. convince the idea. Y.Z. develops the theory, and Q.W. implements it with numerical calculations. Y.Z. and Q.W. contribute equally to this work. H.W., X.Y. and S.S. analyze the data. All authors contribute to the writing of the paper.

COMPETING INTERESTS

The authors declare no competing interests.

ADDITIONAL INFORMATION

Supplementary information The online version contains supplementary material available at https://doi.org/10.1038/s41534-022-00642-z.

Correspondence and requests for materials should be addressed to Yuan Zhang, Chongxin Shan or Klaus Mølmer.